Am J Cancer Res 2024;14(3):1033-1051
www.ajcr.us /ISSN:2156-6976/ajcr0154727

Original Article

Higher overall survival rates of oral squamous cell carcinoma treated with metronomic neoadjuvant chemotherapy

Shinichiro Kina[1], Sho Miyamoto[2], Reika Kawabata-Iwakawa[3], Mika Kina-Tanada[4], Masaru Ogawa[4], Satoshi Yokoo[4]

[1]Department of Medical Education and Development, Graduate School of Medicine, Gunma University, Maebashi, Gunma, Japan; [2]Department of Oral Surgery, Sapporo Medical University School of Medicine, South-1, West-16, Chuo-ku, Sapporo, Hokkaido, Japan; [3]Division of Integrated Oncology Research, Gunma University Initiative for Advanced Research, Gunma University, Maebashi, Gunma, Japan; [4]Department of Oral and Maxillofacial Surgery and Plastic Surgery, Graduate School of Medicine, Gunma University, Maebashi, Gunma, Japan

Received December 2, 2023; Accepted March 2, 2024; Epub March 15, 2024; Published March 30, 2024

Abstract: Distant metastasis is an important prognostic factor for oral squamous cell carcinoma (OSCC). It involves the direct spread of tumor cells through blood vessels or via lymph nodes; however, there are currently no well-established treatments for its prevention in patients with OSCC. To investigate the impact of metronomic neoadjuvant chemotherapy on OSCC, we conducted a retrospective analysis of the efficacy of neoadjuvant chemotherapy with S-1 alone. Fifty-four patients underwent up-front surgery, while 106 received neoadjuvant chemotherapy with S-1 alone. A serious adverse event occurred in one of patient treated with neoadjuvant chemotherapy (1%); however, all patients underwent resection. The 5-year overall survival rate was higher with S-1 than with up-front surgery (96% vs. 81%, P = 0.002). Moreover, neoadjuvant chemotherapy significantly increased the overall survival rate of patients with poorly or moderately differentiated tumors, but not those with well-differentiated tumors. By analyzing a cohort of 523 head and neck squamous cell carcinoma (HNSCC) patients in the Cancer Genome Atlas, we identified genetic variants associated with histological differentiation. The frequency of pathogenic/likely pathogenic variants or deletions in 5 genes associated with HNSCC correlated with histological differentiation, some of which indicated the activation of the Wnt/β-catenin pathway in well-differentiated HNSCC. The vessel marker CD31 was highly expressed in poorly differentiated OSCC, whereas the anti-angiogenic molecule, LCN2, which is induced by the activation of the Wnt pathway, was highly expressed in well-differentiated OSCC. The present study showed that overall survival rates were higher in patients with poorly or moderately differentiated OSCC who received metronomic neoadjuvant chemotherapy, which was attributed to a difference in angiogenesis based on the characteristic landscape of pathogenic mutations according to histological differentiation.

Keywords: Metronomic neoadjuvant chemotherapy, oral squamous cell carcinoma, histological differentiation, distant metastasis

Introduction

The incidence of oral cancer is increasing worldwide [1, 2]. Oral squamous cell carcinoma (OSCC) accounts for more than 80% of oral cancers [3]. Among OSCC recurrences, distant metastasis, once it occurs, is difficult to cure completely [4]. It involves the direct spread of tumor cells through blood vessels or via lymph nodes [5]. A number of studies on neoadjuvant chemotherapy with cisplatin at maximum tolerated doses (MTD) failed to demonstrate survival benefits in OSCC patients [6]. Therefore, the development of treatments that prevent distant metastasis is needed to improve the survival of OSCC patients.

In the past decade, the blockade of angiogenesis has emerged as an effective and promising therapeutic approach for a number of malignancies. CD31 is expressed in tumor microvessels [7], and its expression negatively correlates with prognosis and survival [8]. Metronomic chemotherapy (the continuous and

https://doi.org/10.62347/EYNT8387

low-dose administration of chemotherapeutic agents) was found to exert anti-angiogenic effects by reducing the expression of CD31 in the nude mouse tumor-bearing model of the OSCC cell line, HSC2 [9]. Metronomic adjuvant chemotherapy was shown to significantly improve the overall survival of patients with advanced OSCC in a randomized study in China [10], but not that of patients with advanced OSCC in a randomized study in India [11]. Therefore, the benefits of metronomic chemotherapy for OSCC remain controversial. The stratification of patients to identify those who will benefit from metronomic chemotherapy is critical for the rational design of metronomic chemotherapy.

The neoadjuvant blockade of angiogenesis has been shown to markedly suppress distant metastasis in several tumor types and strongly correlated with improved survival [12]. Its suppressive effects on distant metastasis may be attributed to synergy of a higher microvessel density with the inhibition of angiogenesis [13]. Furthermore, recent studies reported the predictive value of baseline serum LCN2 levels for progression-free survival following the blockade of angiogenesis in patients with advanced kidney cancer [14]. These findings suggest that serum LCN2 levels have the potential to monitor outcomes in these patients after neoadjuvant treatment to block angiogenesis. Therefore, predictive markers, a more detailed understanding of the mechanisms underlying individual responses to the blockade of angiogenesis, and the rational design of neoadjuvant therapies are important.

Recent advances in oral fluoropyrimidine prodrugs have increased the application of metronomic chemotherapy to the treatment of OSCC, with adjuvant settings being linked to survival improvements [15]. However, a consensus has not yet been reached on the use of neoadjuvant metronomic chemotherapy with these prodrugs to treat OSCC [15]. Furthermore, insufficient clarification of metronomics with maximum tolerated dose chemotherapy in previous studies has prevented the confirmation of effects of metronomic neoadjuvant chemotherapy and identification of patients it is expected to benefit. Mutation biomarkers have gained attention for their potential to predict the prognosis and treatment outcomes in OSCC [16]. Promisingly, integrated genomic analyses in OSCC samples have defined a new molecular subtype of OSCC [17]. Although, OSCC molecular subtypes are not associated with clinical staging systems, integrating molecular and genomic information plays an important role for developing new approaches for future therapeutic strategies [18]. However, the survival outcome of OSCC patients with S-1 monotherapy has not been explored thoroughly. Given the widespread use of mutation check, we tried to identify mutation biomarker candidates applicable within clinical settings for guiding the choice of metronomic neoadjuvant chemotherapy with S-1. The present study investigated the effects of neoadjuvant chemotherapy with S-1 alone in patients with OSCC and examined the genetic landscape of HNSCC to identify patients who will benefit from metronomic chemotherapy.

Methods

Patients

The Ethics Committee of Gunma University approved the present study (approval number HS2017-142), and all patients provided their written informed consent. Patients diagnosed with OSCC between 7 October 2009 and 10 January 2017 were extracted from the database of Gunma University Hospital. Eligible patients were ≥18 years and had previously untreated, histologically confirmed OSCC.

Exclusion criteria

1. Male or female >75 years at the first visit. 2. Hemoglobin ≤8.5 g dl^{-1}. 3. Absolute neutrophil count (ANC) ≤1.5 × 10^9 L^{-1} (≤1,500 per mm^3). 4. Platelet count ≤50 × 10^9 L^{-1} (≤500,000 per mm^3). 5. ALT>3 × ULN. 6. Total bilirubin >2.5 mg/dL.

Study design

We conducted a retrospective, single institutional study to assess the efficacy and safety of neoadjuvant chemotherapy with S-1, an oral fluoropyrimidine anticancer agent, in patients with OSCC. In our institute, surgery without neoadjuvant chemotherapy is preferred for the treatment of OSCC; however, patients for whom surgery was not available because of a busy schedule received neoadjuvant chemotherapy with S-1 alone. Patients received 120 mg of S-1 orally twice daily for 2 weeks or underwent upfront surgery. This dose is consistent with that used in an efficacy trial for gastric cancer [19].

Endpoints

The primary endpoint was overall survival, defined as the time to death from any cause in a 5-year period. Secondary efficacy endpoints during the 5-year period were disease-free survival, the time to first recurrence, local recurrence, regional recurrence, distant metastasis, and death from any cause. Survival endpoints were described using the Kaplan-Meier method. Data on patients who remained alive and free of disease were censored at the date of the last follow-up. Safety was assessed based on blood testing. Adverse events (AE) were recorded. The documented severity of AE was classified according to the Common Terminology Criteria for Adverse Events (grade 1 = mild; grade 2 = moderate; grade 3 = severe; grade 4 = life-threatening; grade 5 = death). The baseline clinical staging of primary tumors and lymph nodes was performed according to the 7th edition of the AJCC Cancer Staging Manual.

Cell culture

The HSC4 (RIKEN), HSC3 (Japanese Collection of Research Bioresources: JCRB), SCC4 (JCRB), HO-1-u-1 (RIKEN), OSC19 (JCRB), and HSC2 (JCRB) cell lines used for in vitro experiments in the present study were all derived from OSCC patients. Cells were cultured at 37°C and 5% CO_2 and grown in DMEM (WAKO) or F-12 medium (WAKO) supplemented with 10% FBS (Biological Industries) and 1% penicillin-streptomycin (WAKO).

Protein blotting

Cells were harvested and lysed in Laemmli sample buffer (Bio-Rad). Total protein in each sample was loaded onto an SDS-PAGE gel, separated, and transferred to a polyvinylidene fluoride membrane (Bio-Rad). The membrane was blocked and then incubated with a β-catenin antibody (1:1,000 dilution, Santa Cruz Biotechnology), LCN2 antibody (1:1,000 dilution, Abcam), β-actin antibody (1:5,000 dilution, Sigma-Aldrich), and anti-mouse secondary antibody (1:5,000 dilution, ProteinTech). Membranes were scanned using LAS4010 (GE Healthcare).

Immunohistochemistry

To evaluate LCN2 and ICAM1 protein expression according to histological differentiation, immunohistochemistry was performed using standard techniques as previously described [30]. Biopsies were fixed in paraformaldehyde and embedded in paraffin by the pathology laboratory. Four-micron-thick slices were cut from FFPE tumor samples. Briefly, slides were deparaffinized using ImmunoSaver at 95°C for 25 min. After cooling, slides were washed in TBS twice for 5 min. Blocking of endogenous peroxidase and non-specific antibody binding (in 1× PBS containing 0.1% Triton X-100 and 2% BSA) was performed. Tissue sections were then stained with a LCN2 antibody (1:50 dilution, R&D Systems) and an ICAM1 antibody (1:50 dilution, Santa Cruz) at room temperature for 30 min. Histofine Simple Stain MAX PO HRP polymers (424131, Nichirei) were added at room temperature for 15 min after washing twice. DAB (425011, Nichirei) was then added to samples for 5 min. After washing twice, slides were permanently mounted. Slides were scanned up to ×40 magnification.

Wnt inhibitor treatment

Wnt974 (Selleck) was added to the culture medium at a concentration of 0.01 mM and cells were harvested 48 hours later. Total RNA was extracted using ISOGEN reagent (NIPPON GENE) and then reverse transcribed to cDNA. Real-time PCR was performed using SYBR Green Supermix (Bio-Rad). LCN2 expression levels were normalized to the corresponding β-actin values and shown as a fold change from the value of the control sample (the ΔΔCt method). Sample analyses were performed in duplicate. In quantitative real-time PCR, we used the primers 5'-CAAGGAGCTGACTTCGGAAC-3' (sense) and 5'-TACACTGGTCGATTGGGACA-3' (antisense) for LCN2 and 5'-CTGGAACGGTGAAGGTGACA-3' (sense) and 5'-AAGGGACTTCCTGTAACAACGC-3' (antisense) for human β-actin mRNA. Quantitative real-time PCR was conducted using the SYBR® Green PCR Master Mix (Applied Biosystems) and ABI Real-Time PCR Step One Plus.

Statistical analysis

Fisher's exact test was used to compare categorical variables. Survival curves were compared using the Log-rank test. Survival and disease-free survival were measured from the first visit. An OSCC event analysis was performed using death as a competing risk. A mul-

tivariate logistic regression analysis was used to assess prognostic factors associated with regional recurrence and the development of distant metastasis. A multivariable Cox proportional hazards model was employed to assess prognostic factors associated with overall survival. Relationships were assessed using Spearman's correlation coefficient. *P* values <0.05 were considered to be significant. All analyses were performed using the statistical software JMP version 15. Box plots were generated using Microsoft excel.

Results

Patients

We extracted patients with OSCC between October 7, 2009 and January 14, 2017 from the database of the Gunma University Hospital. OSCC was diagnosed based on clinical and histopathological criteria. The clinical tumor node metastasis (cTNM) status of tumors was classified based on CT and neck ultrasonography. A total of 106 patients received neoadjuvant chemotherapy with S-1 alone and 54 underwent up-front surgery (**Table 1**). Ten patients were lost to the follow-up. No significant differences were observed in the clinical characteristics of patients between the neoadjuvant and surgery groups (P>0.05, the χ-squared test; **Table 1**). Therefore, 160 patients underwent surgery or received neoadjuvant chemotherapy with S-1 and were evaluable for safety as well as primary and secondary efficacy endpoints (**Figure 1**).

Primary and secondary endpoints

Survival-related clinicopathological features, including tumor stage, poorly or moderately differentiation and neoadjuvant chemotherapy with S-1, exhibited the significant associations with overall survival (OS) (**Figure 2A**). The 5-year overall survival rate (the primary endpoint) was 96% in the S-1 group and 81% in the surgery group (P = 0.002) (**Figure 2B**), while the 5-year disease-free survival rate was 91% in the S-1 group and 70% in the surgery group (P = 0.0002) (**Figure 2C**).

Safety

One safety concern (1%) was identified (**Table 2**).

Cumulative incidence of local recurrence, regional recurrence, and the development of distant metastasis

Among 160 patients, 3 (6%) in the surgery group and 4 (4%) in the S-1 group had local recurrence, while 9 patients (17%) in the surgery group and 2 (2%) in the S-1 group had regional recurrence. Among all 160 patients, patients in the neoadjuvant chemotherapy with S-1 group had a significantly lower cumulative incidence of regional recurrence than those in the surgery group (P = 0.0004), and the cumulative incidence of local recurrence was similar between the S-1 and surgery groups (P = 0.6) (**Figure 3A**, **3B**). Seven of the 54 patients in the surgery group and 2 of the 106 patients in the S-1 group had distant metastasis. The cumulative incidence of distant metastasis was significantly lower in the S-1 group than in the surgery group (1.9% vs. 13.0%, P = 0.004) (**Figure 3C**).

Clinical characteristics of patients with and without regional recurrence or distant metastasis

To examine the characteristics of patients with regional recurrence or distant metastasis, we compared the contribution rate of clinical characteristics between patients with and without regional recurrence or distant metastasis. Twenty-five of the 149 patients without regional recurrence (16.8%) and 25 of the 151 patients without distant metastasis (16.6%) had poorly or moderately differentiated tumors (**Tables 3** and **4**). Patients with regional recurrence or distant metastasis had a significantly higher contribution of poorly or moderately differentiation (5/11, 45.5%) and (5/9, 55.6%), respectively. The frequency of poorly or moderately differentiated tumors was significantly higher in patients with than in those without regional recurrence or distant metastasis. Furthermore, in the multivariate analysis of regional recurrence and the incidence of distant metastasis in patients with stage I-III disease, only poor or moderate differentiation was identified as a significant prognostic factor for an increased risk of recurrence (Regional recurrence: HR 5.82, 95% CI 1.46-23.24, P<0.05, Development of distant metastasis: HR 6.52, 95% CI 1.39-30.43, P<0.05) (**Tables 5**, **6**). Clinical risk factors traditionally used for staging and prog-

Table 1. Baseline characteristics of patients*

Characteristics	Neoadjuvant chemotherapy with S-1 (N = 106)	Up-front surgery (N = 54)	P
Age - yr	61±13	56±16	0.08
Female sex - no. (%)	41 (38.7)	20 (34.5)	0.9
Primary tumor site			0.4
Tongue	69 (65.0)	38 (70.3)	
Gingiva	19 (17.9)	6 (11.1)	
Floor	5 (4.7)	5 (9.2)	
Other	13 (12.2)	5 (9.2)	
Clinical T stage - no. (%)			0.2
T1	33 (31.1)	17 (31.5)	
T2	60 (56.6)	35 (64.8)	
T3	13 (12.2)	2 (3.7)	
Clinical N stage - no. (%)			0.7
N0	97 (91.5)	51 (94.5)	
N1	9 (8.5)	3 (5.5)	
AJCC clinical stage - no. (%)			0.1
I	33 (31.1)	17 (31.5)	
II	53 (50.0)	33 (61.1)	
III	20 (18.9)	4 (7.4)	
Histological differentiation - no. (%)			0.2
Well	66 (62.3)	35 (64.8)	
Well to moderately	19 (17.9)	4 (7.4)	
Moderately	12 (11.3)	12 (22.2)	
Poorly to moderately	3 (2.8)	1 (1.9)	
Poorly	1 (1.0)	1 (1.9)	
Unknown	5 (4.7)	1 (1.9)	
Body mass index$	22±3	22±4	0.9
Adjuvant chemotherapy - no. (%)	36 (34.0)	11 (20.4)	0.1

AJCC, American Joint Committee on Cancer. *Plus-minus values are means ± SD. Percentages may not total 100 because of rounding. $Data were available for 106 patients in the chemotherapy group and 53 in the surgery group.

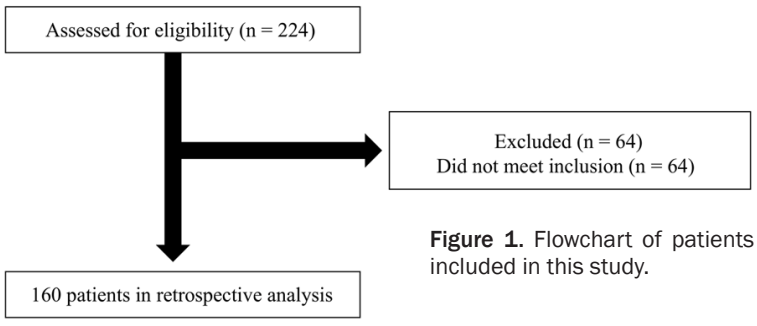

Figure 1. Flowchart of patients included in this study.

nostication were not significant. These results indicate that histological differentiation may affect the primary and secondary endpoints of neoadjuvant chemotherapy with S-1.

Impact of histological differentiation on endpoints

We examined the primary and secondary endpoints of neoadjuvant chemotherapy with S-1 according to histological differentiation in order to confirm whether a relationship existed. In the multivariable analysis of OS in patients with poorly or moderately differentiated tumors, neoadjuvant chemotherapy with S-1 was identified as a significant prognostic factor for a decreased risk of death (HR 0.031, 95% CI 0.002-0.376, P = 6.4 × 10^{-3}) (**Figure 4A**).

A Multivariable analysis of overall survival rate

Factors	HR (95% CI)	*P* value
Neoadjuvant chemotherapy with S-1	0.134 (0.035, 0.511)	3.2×10^{-3}
Adjuvant chemotherapy	0.995 (0.248, 3.990)	0.995
Age (70≦)	2.683 (0.883, 8.151)	8.17×10^{-2}
Male gender	1.749 (0.466, 6.554)	0.406
AJCC Stage (II-III)	13.319 (1.577, 112.426)	1.74×10^{-2}
Poorly or moderately differentiation	8.003 (2.301, 27.835)	1.1×10^{-3}
BMI (25≦)	0.464 (0.0559, 3.854)	0.477

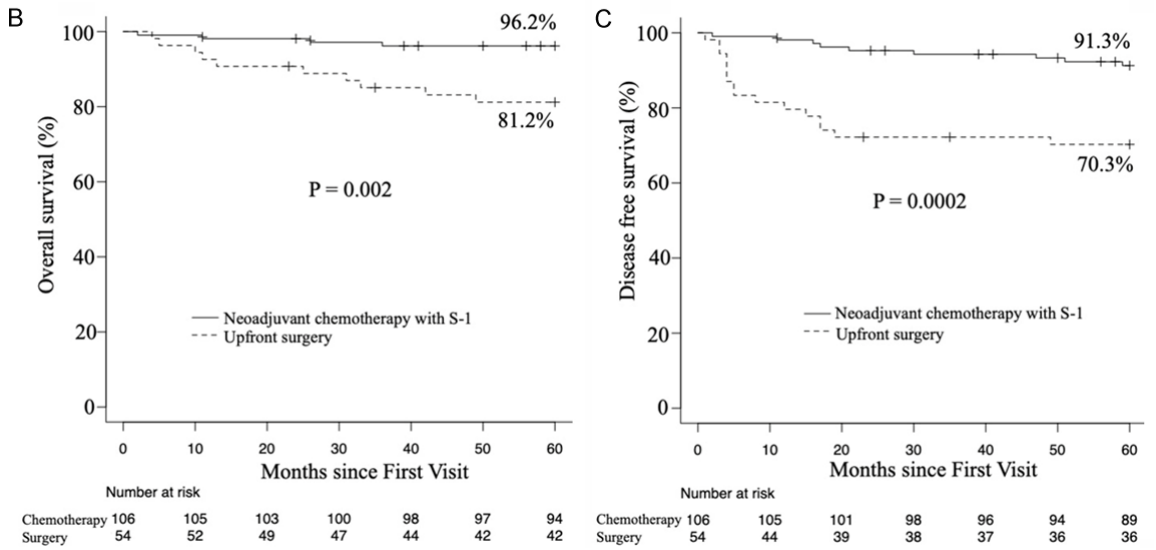

Figure 2. Overall survival and disease-free survival rates. A. Multivariable Cox proportional hazards regression for overall survival rate. The graph shows the HR of the Cox proportional hazards model, with error bars indicating two-sided 95% CIs (Cox regression multivariable analysis). *P* values were calculated using multivariable Cox proportional hazards regression. Two-sided *P* values were calculated. B. The primary endpoint was the 5-year overall survival rate. C. The secondary endpoint was the 5-year disease-free survival rate. Patients received neoadjuvant chemotherapy with S-1 orally or underwent up-front surgery.

Neoadjuvant chemotherapy was not significant in patients with well-differentiated tumors (data not shown). The results obtained showed that neoadjuvant chemotherapy with S-1 significantly increased the overall survival rate of patients with poorly or moderately differentiated OSCC (93.8% in neoadjuvant chemotherapy versus 50.0% in up-front surgery), whereas the overall survival rate of patients with well-differentiated OSCC was similar following neoadjuvant chemotherapy and up-front surgery (95.4% in neoadjuvant chemotherapy versus 91.2% in up-front surgery) (**Figure 4B**). Neoadjuvant chemotherapy with S-1 also significantly increased the disease-free survival rate of patients with poorly or moderately differentiated OSCC (75.0% in neoadjuvant chemotherapy versus 35.7% in up-front surgery) (**Figure 4C**), but not those with well-differentiated OSCC (data not shown). Patients with poorly or moderately differentiated OSCC were previously reported to benefit from neoadjuvant chemotherapy [20].

Genetic characteristics of well-, moderately, and poorly differentiated HNSCC

HNSCC comprises a heterogeneous group of tumors, and its molecular etiology according to histological differentiation is unclear. To identify genetic variants associated with well-differentiated HNSCC, we analyzed the whole-exome sequencing data of a cohort of 523 patients

Table 2. Safety of S-1, number of subjects (%)

	Neoadjuvant chemotherapy with S-1 (N = 106)
Patients with any AE	78 (74)
AE leading to death	0 (0)
Any SAE	1 (1)
AE leading to discontinuation of S-1	20 (19)
White blood cell decrease	30 (28)
Anemia	27 (25)
Thrombocytopenia	26 (25)
Bilirubin increase	19 (18)
Pruritus	8 (8)
ALT increase	9 (8)

AE, adverse event; SAE, serious adverse event.

with HNSCC in the Cancer Genome Atlas (TCGA) database. Variant pathogenicity in causative genes was evaluated by TCGA. Pathogenic (P) or likely pathogenic (LP) variants were identified across 43 known genes detected in more than five cases (**Figure 5A**). To examine the genetic features of histological differentiation, we compared the contribution rate (defined as the percentage of cases) of P/LP variants between patients with well-, moderately and poorly differentiated HNSCC. *FAT1* had the second highest prevalence of pathogenic alleles, which was previously shown to be specifically mutated in well-differentiated cutaneous cell carcinoma [21]. *FAT1, HRAS, CASP8,* and *FBXW7* emerged as specifically mutated genes in patients with well-differentiated HNSCC (19/63, 30%: 9/63, 14%: 9/63, 14%: 7/63, 11% respectively) (**Figure 5B**), whereas none of pathogenic or likely pathogenic variants were significantly frequently observed in patients with poorly differentiated HNSCC. The combination of *FAT1* and *CASP8* mutations was previously shown to consist of a distinct cluster in HNSCC [22]. Patients with well-differentiated HNSCC had a significantly higher contribution rate of the *CDKN2A* deletion (28/63, 44%) than those with moderately differentiated HNSCC (93/308, 30%) or poorly differentiated HNSCC (33/123, 27%) (**Figure 5C**), which resulted in an increase in the mRNA expression of *CDKN2A* in poorly or moderately differentiated HNSCC (**Figure 5D**). Genes frequently mutated or deleted in well-differentiated HNSCC were implicated in Wnt/β-catenin signaling (**Figure 5E**). The expression of Wnt/β-catenin signaling-related genes, such as Wnt7A and Wnt4, was higher in patients with well-differentiated HNSCC enriched P/LP (*HRAS*) variants or with the *CDKN2A* deletion (**Figure 4E**). *FAT1* and *FBXW7* have been implicated in the degradation of β-catenin [23]. The P/LP variants in *FAT1, HRAS, CASP8,* and *FBXW7* or *CDKN2A* deletions were detected in 43 patients, yielding a 68% contribution to the incidence of well-differentiated HNSCC (**Figure 5F**). These results extended the phenotypic spectrum of genes known to cause HNSCC.

Identification of the timing of mutations in genes involved in the pathogenesis of HNSCC

With the aim of identifying candidate biomarkers that guide the selection of metronomic chemotherapy, we investigated the timing of mutations in genes associated with the pathogenesis of well-differentiated HNSCC. Mutations that occur early are attractive candidate biomarkers. We compared P/LP allele frequencies obtained from the TCGA database. In the tumor evolution model (clonal vs. subclonal variants), allele frequency was associated with the timing of mutations [24]. We examined differences in allele frequencies between mutated genes using the two-sided Student's t-test. *FBXW7* had a significantly higher frequency of P/LP alleles in HNSCC (**Figure 6A**). The *FBXW7* gene was not previously implicated in patients with early HNSCC. *FBXW7* with higher allele frequencies was predicted to be mutated early in the development of well-differentiated HNSCC. Taken together, the *FBXW7* gene was identified as early driver genes in the tumorigenesis of well-differentiated HNSCC.

We also investigated their combinations using the two-sided Fisher's exact test. The combination of P/LP variants across different genes is shown in **Figure 6B.** The loss of chromosome arm 9p (at which *CDKN2A* resides) occurs in the early stage of the tumorigenesis of HNSCC [25]. The co-occurrence of *FAT1* P/LP variants with P/LP variants was significant in *HRAS* (1.90×10^{-3}), *CASP8* (8.80×10^{-3}), and *FBXW7* (4.17×10^{-2}) (**Figure 6B**). *FAT1* encodes a cadherin-like protein, through which

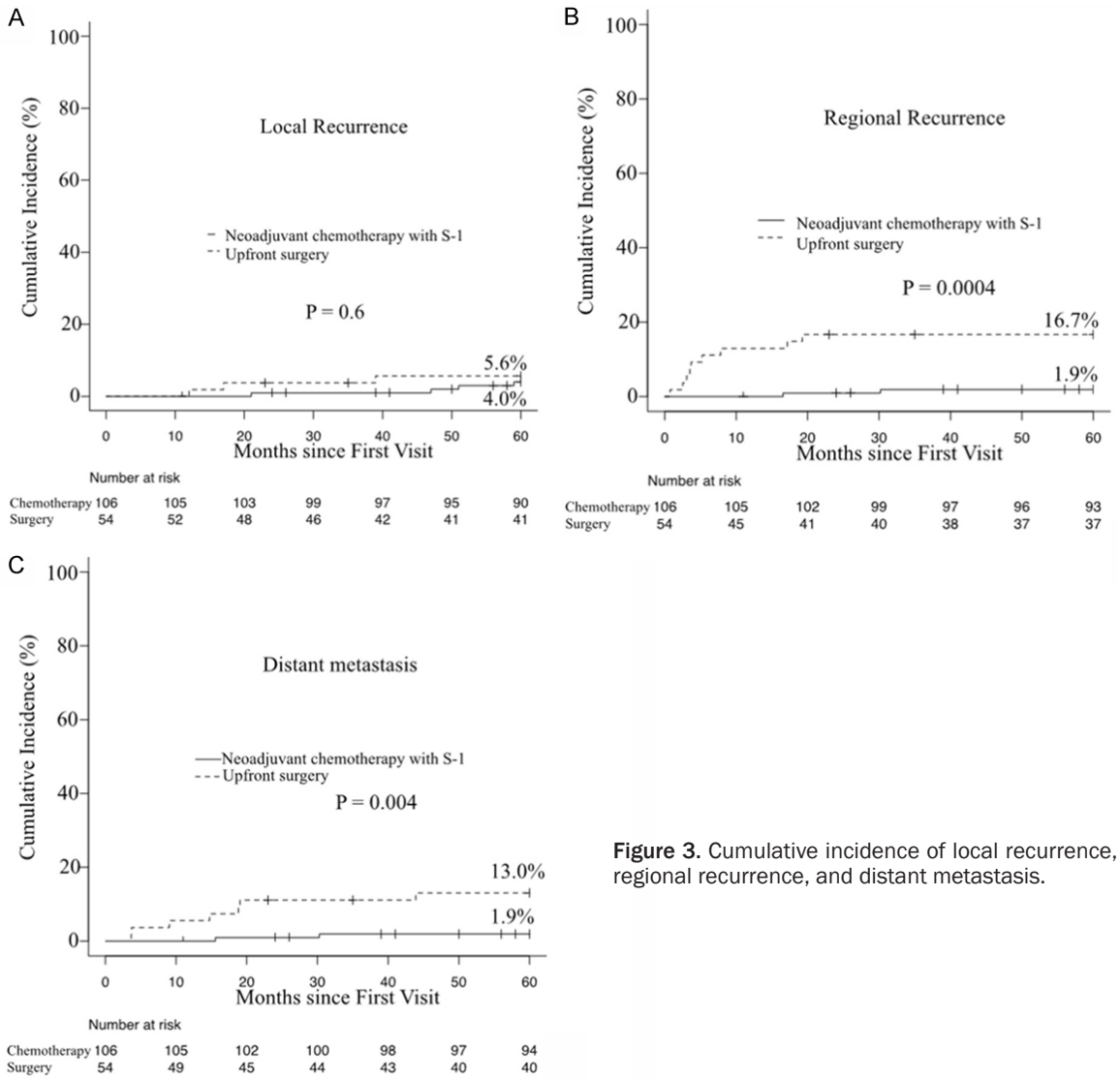

Figure 3. Cumulative incidence of local recurrence, regional recurrence, and distant metastasis.

it interacts with β-catenin. All of the P/LP variants were predicted to disrupt the C-terminal intracellular domain of this protein, thereby impeding its ability to suppress Wnt/β-catenin signaling [26]. The knockout of *FAT1* and *CASP8* in OSCC cells was previously shown to increase terminal differentiation [27]. Other enriched genes in well-differentiated HNSCC, namely, *HRAS, CASP8, CDKN2A*, and *FBXW7*, have been implicated in Wnt ligand expression (**Figure 5E**) or β-catenin activation [28-31].

Enriched Wnt/β-catenin pathway-related genes in well-differentiated HNSCC

Wnt/β-catenin signaling plays an important role in the pathogenesis of HNSCC. β-catenin targets a crucial transcriptional regulator that is required for tumor development [32]. Western blotting revealed the high expression of β-catenin in well-differentiated OSCC cell lines and low expression in poorly differentiated OSCC cell lines (**Figure 6C**).

In addition, the expression of Wnt/β-catenin-related genes (Wnt7A, Wnt4) was significantly enriched in well-differentiated HNSCC (**Figure 6D**). Wnt7A and Wnt4 have been shown to trigger the migration of OSCC and the transcriptional activation of β-catenin-related genes [33, 34]. Some missense variants in Wnt7A and Wnt4 were found in the HNSCC TCGA database (data not shown), whereas no P/LP variants were identified.

Data on 5 genes frequently mutated or deleted in well-differentiated HNSCC suggest their considerable relevance to well-differentiated

Table 3. Demographic and clinical characteristics of patients with regional recurrence

Patients	Patients with regional recurrence 11	Patients without regional recurrence 149	*P* value
Age (y)	60±15	59±14	0.9
Sex, female/male	3/8	58/91	0.74
BMI (kg/m^2)	22.3±4.6	22.1±3.2	0.88
AJCC stage			0.3
I	5/11 (45.5)	45/149 (30.2)	
II	6/11 (54.5)	80/149 (53.7)	
III	0/11 (0)	24/149 (16.1)	
Histological differentiation			0.03
Poorly or moderately	5/11 (45.5)	25/149 (16.8)	
Other	6/11 (54.5)	124/149 (83.2)	
Adjuvant chemotherapy	2/11 (18.2)	45/149 (30.2)	0.5

Table 4. Demographic and clinical characteristics of patients with developing distant metastasis

Patients	Patients with developing distant metastasis 9	Patients without developing distant metastasis 151	*P* value
Age (y)	59±14	59±14	0.89
Sex, female/male	1/8	60/91	0.15
BMI (kg/m^2)	22.9±3.7	22.1±3.3	0.47
AJCC stage			0.13
I	1/9 (11.1)	49/151 (32.5)	
II	8/9 (88.9)	78/151 (51.7)	
III	0/9 (0)	24/151 (15.9)	
Histological differentiation			0.012
Poorly or moderately	5/9 (55.6)	21/151 (16.6)	
Other	4/9 (44.4)	126/151 (83.4)	
Adjuvant chemotherapy	5/9 (55.6)	42/151 (27.8)	0.13

HNSCC development (**Figure 6E**). These results strongly suggest that these 5 genes are previously unrecognized causative genes of well-differentiated HNSCC.

Angiogenesis-related gene expression according to histological differentiation

Distant metastasis or chemotherapy resistance correlated with tumor microvessel density. CD31 is expressed at high levels on endothelial cells and is often used as a tumor neovascular endothelial marker [35]. CD31 protein expression positively correlated with histological differentiation (**Figure 7A**), which revealed the higher microvessel densities of poorly or moderately differentiated tumors [36]. Immunohistochemistry staining of CD31+ cells from biopsy of well and poorly differentiated OSCC, confirmed an increase of immature blood vessels lacking lumen in poorly differentiated OSCC (**Figure 7B**). ICAM1, intercellular adhesion molecule 1, crucial for tumor cell-endothelial cell adhesion in endothelial cells during distant metastasis [37], expression also positively correlated with histological differentiation ($P = 5.09 \times 10^{-8}$) (**Figure 7C**). Immunohistochemistry staining of ICAM1+ cells from biopsy of OSCC, confirmed mild increase of ICAM1 positive endothelial cells in core area of tumors according to histological differentiation (**Figure 7D**). We performed transcriptional and immunohistochemical analyses of a previously proposed biomarker of responses to chemotherapy and angiogenesis blockade therapy, Lcn2 [14, 38], which is associated with anti-angiogenesis [39]. The expression of the potential predictive biomarker and angiogenesis suppressor, LCN2 [39] negatively correlated with

Table 5. A multivariate analysis of regional recurrence in patients with stage I-III OSCC

Risk factors	Univariate Analysis		Multivariate Analysis	
	OR (95% CI)	*P* value	OR (95% CI)	*P* value
Age (70≤)	1.17 (0.29-4.67)	0.81	1.07 (0.25-4.50)	0.92
Male gender	1.69 (0.43-6.66)	0.43	1.60 (0.39-6.59)	0.5
BMI (25≤)	2.41 (0.59-9.88)	0.21	2.77 (0.61-12.61)	0.18
AJCC stage (II-III)	0.51 (0.15-1.78)	0.29	0.72 (0.18-2.79)	0.64
Poorly or moderately differentiation	4.13 (1.16-14.60)	0.02	5.82 (1.46-23.24)	0.012
Adjuvant chemotherapy	0.51 (0.10-2.47)	0.37	0.33 (0.05-1.97)	0.22

Various prognostic factors and their relationship with regional recurrence, as indicated by OR, were analyzed across the cohort.

Table 6. A multivariate analysis of the development of distant metastasis in patients with stage I-III OSCC

Risk factors	Univariate Analysis		Multivariate Analysis	
	OR (95% CI)	*P* value	OR (95% CI)	*P* value
Age (70≤)	0.37 (0.01-2.12)	0.3	0.28 (0.03-2.54)	0.25
Male gender	5.27 (0.64-43.25)	0.12	7.11 (0.78-64.31)	0.08
BMI (25≤)	1.76 (0.34-9.09)	0.49	2.39 (0.36-15.83)	0.36
AJCC stage (II-III)	3.84 (0.46-31.59)	0.21	4.55 (0.44-47.00)	0.2
Poorly or moderately differentiation	6.30 (1.58-25.11)	0.009	6.52 (1.39-30.43)	0.01
Adjuvant chemotherapy	3.24 (0.83-12.66)	0.09	1.55 (0.31-7.53)	0.58

Various prognostic factors and their relationship with regional recurrence, as indicated by OR, were analyzed across the cohort.

histological differentiation (**Figure 7E**). Immunohistological staining revealed higher LCN2 protein expression levels in well-differentiated tumors than in poorly or moderately differentiated tumors (**Figure 7F**), which was consistent with previous findings showing the specific expression of LCN2 in well-differentiated pancreatic cancer [39]. An immune infiltration analysis using the Timer 2.0 database revealed that the expression of LCN2 negatively correlated with the infiltration of endothelial cells (**Figure 7G**), indicating its suppressive functions on angiogenesis and neovascularization around well-differentiated HNSCC. In addition, LCN2 mRNA expression decreased after a treatment with the Wnt inhibitor, Wnt974 (**Figure 7H**) and LCN2 protein expression was reduced in Wnt974-treated OSC19 cells (**Figure 7I**), suggesting that the activation of Wnt plays a role in the up-regulation of LCN2 and suppression of angiogenesis.

Gene sets associated with poorly differentiated HNSCC

Even if none of the genes in poorly differentiated HNSCC had a significantly higher percentage of P/LP as in well-differentiated tumors, the cumulation of non-significant genes but having mild trends may still be informative when prioritizing candidate genes as relevant or increasing susceptibility to poorly differentiated HNSCC. Among genes that were amplified, *CCND1* (P = 0.123) emerged as a potentially relevant gene (**Figure 8A**). An analysis of variants of uncertain significance (VUSs) provides insights into the pathogenesis of poorly differentiated HNSCC. Therefore, we analyzed VUSs that may be relevant to poorly differentiated HNSCC, and the results obtained are shown in **Figure 8B**, **8C**. *NAV3* and *ASPM* were specifically mutated in poorly differentiated HNSCC (**Figure 8B**). VUSs in *NAV3* and *ASPM* had significantly lower Wnt7A expression levels ($P = 4.0 \times 10^{-2}$ and $P = 4.9 \times 10^{-2}$, respectively), indicating Wnt inhibitory roles in poorly differentiated HNSCC (**Figure 8C**) [40]. Moreover, aneuploidy scores ($P = 2.8 \times 10^{-3}$) (**Figure 8D**) were significantly higher in poorly or moderately differentiated HNSCC, suggesting a relationship between aneuploidy and sensitivity to metronomic chemotherapy. This result indicates the benefits of a karyotype analysis of patients receiving metronomic neoadjuvant chemotherapy.

A

Multivariable analysis of overall survival rate of patients with poorly or moderately differentiated OSCC

Factors	HR (95% CI)	*P* value
Neoadjuvant chemotherapy with S-1	0.031 (0.002, 0.376)	6.4×10^{-3}
Adjuvant chemotherapy	0.563 (0.075, 4.196)	0.575
Age (70≦)	2.052 (0.364, 11.555)	0.414
Male gender	0.567 (0.083, 3.849)	0.561
AJCC Stage (II-III)	21.452 (1.933, 238.046)	1.25×10^{-2}
BMI (25≦)	1.160 (0.093, 14.395)	0.907

B

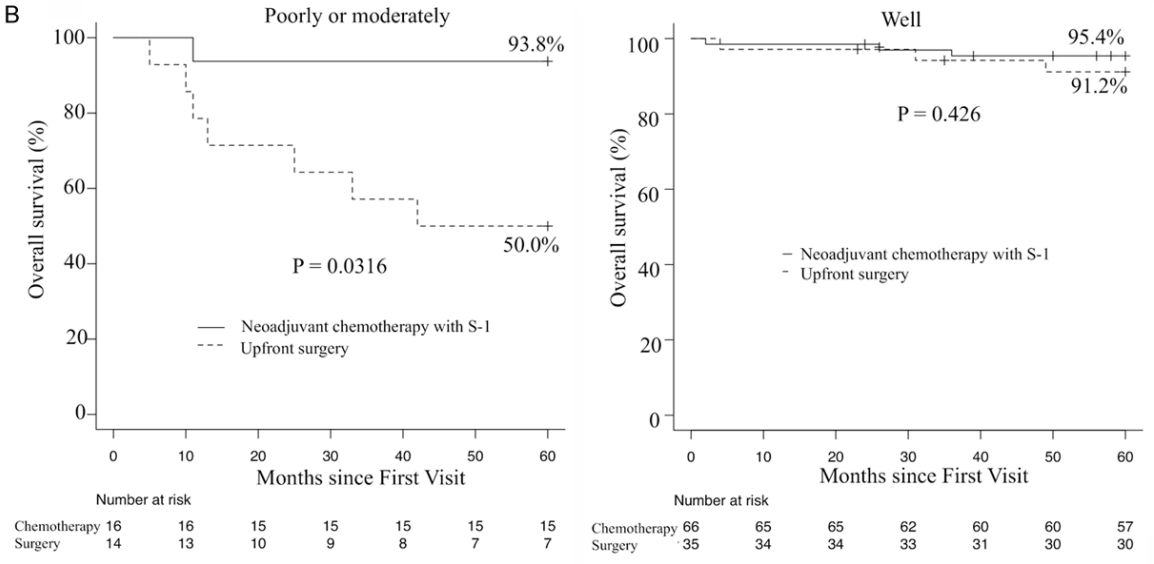

C

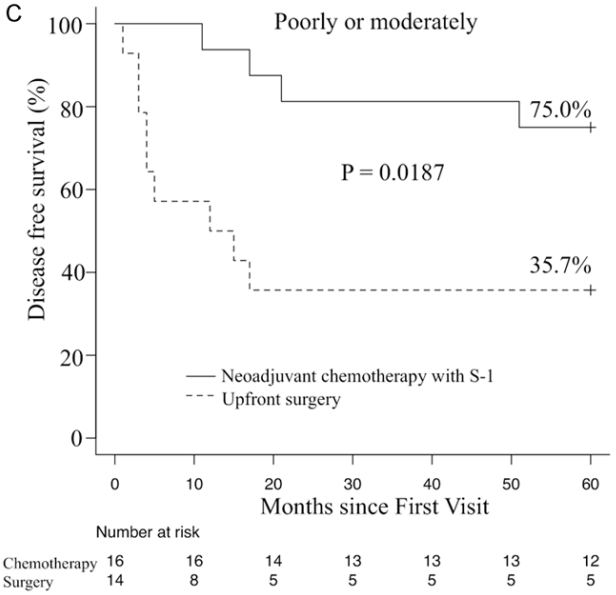

Figure 4. Primary outcome according to histological differentiation. A. Multivariable Cox proportional hazards regression for overall survival rate of patients with poorly or moderately differentiated OSCC. The graph shows the HR of the Cox proportional hazards model, with error bars indicating two-sided 95% CIs (Cox regression multivariable analysis). *P* values were calculated using multivariable Cox proportional hazards regression. Two-sided *P* values were calculated. B. Kaplan-Meier survival curves comparing OS between patients receiving neoadjuvant chemotherapy with S-1 and up-front surgery. Poorly or moderately differentiation (left) and well-differentiation (right). *P* values were calculated using the log-rank test. C. Kaplan-Meier survival curves comparing disease-free survival between poorly or moderately differentiated OSCC patients receiving neoadjuvant chemotherapy with S-1 and up-front surgery. *P* values were calculated using the log-rank test.

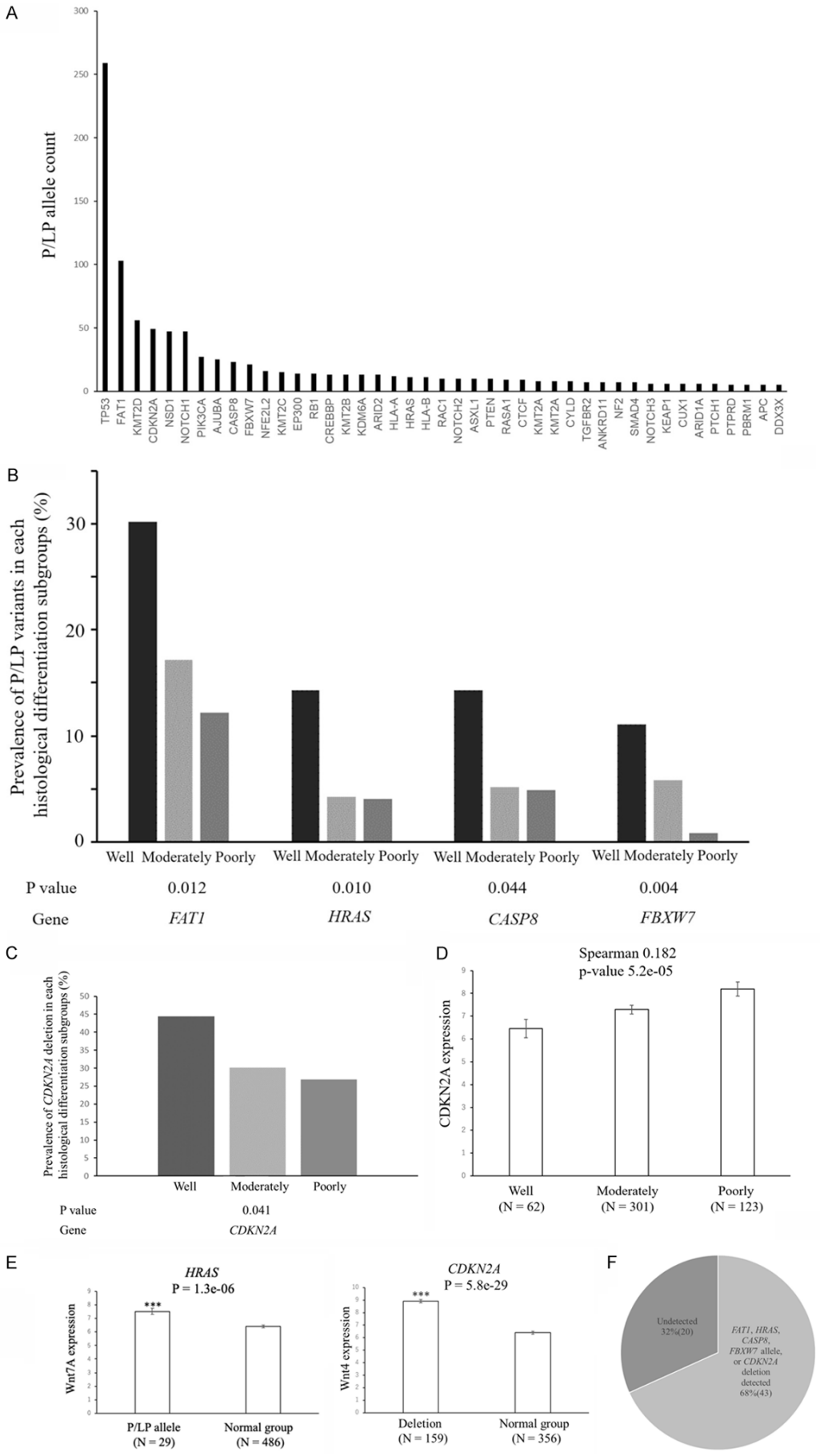
A
P/LP allele count
TP53 FAT1 KMT2D CDKN2A NSD1 NOTCH1 PIK3CA AJUBA CASP8 FBXW7 NFE2L2 KMT2C EP300 RB1 CREBBP KMT2B KDM6A ARID2 HLA-A HRAS HLA-B RAC1 NOTCH2 ASXL1 PTEN RASA1 CTCF KMT2A KMT2A CYLD TGFBR2 ANKRD11 NF2 SMAD4 NOTCH3 KEAP1 CUX1 ARID1A PTCH1 PTPRD PBRM1 APC DDX3X
B
Prevalence of P/LP variants in each histological differentiation subgroups (%)
Well Moderately Poorly Well Moderately Poorly Well Moderately Poorly Well Moderately Poorly
P value 0.012 0.010 0.044 0.004
Gene FAT1 HRAS CASP8 FBXW7
C
Prevalence of CDKN2A deletion in each histological differentiation subgroups (%)
Well Moderately Poorly
P value 0.041
Gene CDKN2A
D
Spearman 0.182
p-value 5.2e-05
CDKN2A expression
Well (N = 62) Moderately (N = 301) Poorly (N = 123)
E
HRAS
P = 1.3e-06
Wnt7A expression
P/LP allele (N = 29) Normal group (N = 486)
CDKN2A
P = 5.8e-29
Wnt4 expression
Deletion (N = 159) Normal group (N = 356)
F
Undetected 32%(20)
FAT1, HRAS, CASP8, FBXW7 allele, or CDKN2A deletion detected 68%(43)

Figure 5. Overview of P/LP variants enriched in HNSCC genes. A. Allele counts of P/LP variants detected in 43 known HNSCC genes. B. P/LP variants in 4 genes were enriched in well-differentiated HNSCC relative to other differentiated HNSCC (well-differentiated cases n = 63; moderately differentiated cases n = 308; poorly differentiated cases n = 123). Genes with P<0.05 are shown. The graph shows the contribution rate of each P/LP variant in patients with different histological differentiation. *P* values for differences in the prevalence of P/LP variants between well-differentiated cases and other cases are generated by two-sided Fisher's exact tests. C. The contribution rate of the *CDKN2A* deletion according to the histological differentiation of HNSCC. A deletion in the *CDKN2A* gene was enriched in well-differentiated HNSCC relative to other differentiated HNSCC (well-differentiated cases n = 63; moderately differentiated cases n = 308; poorly differentiated cases n = 123). Genes with P<0.05 are shown. The graph shows the contribution rate of each *CDKN2A* deletion in patients with different histological differentiation. *P* values for differences in the prevalence of the *CDKN2A* deletion between well-differentiated cases and other cases are generated by two-sided Fisher's exact tests. D. Relationship between histological differentiation and *CDKN2A* expression in head and neck cancers. The RSEM values for *CDKN2A* are shown for head and neck cancers from the TCGA dataset. Data are shown as means ± s.e.m. *CDKN2A* expression positively correlated with histological differentiation using Spearman's rank-based correlation. E. Relationship between P/LP variants or deletions and Wnt/β-catenin signaling-related gene expression in head and neck cancers. RNA-Seq by Expectation-Maximization (RSEM) values for Wnt7A and Wnt4 are shown for head and neck cancers from the TCGA dataset. Data are shown as means ± s.e.m. A two-sided t-test was used to assess significance. Numbers indicate *P*-values. *P<0.05, ***P<0.001. F. The contribution of well-differentiation-specific genes in 63 well-differentiated cases.

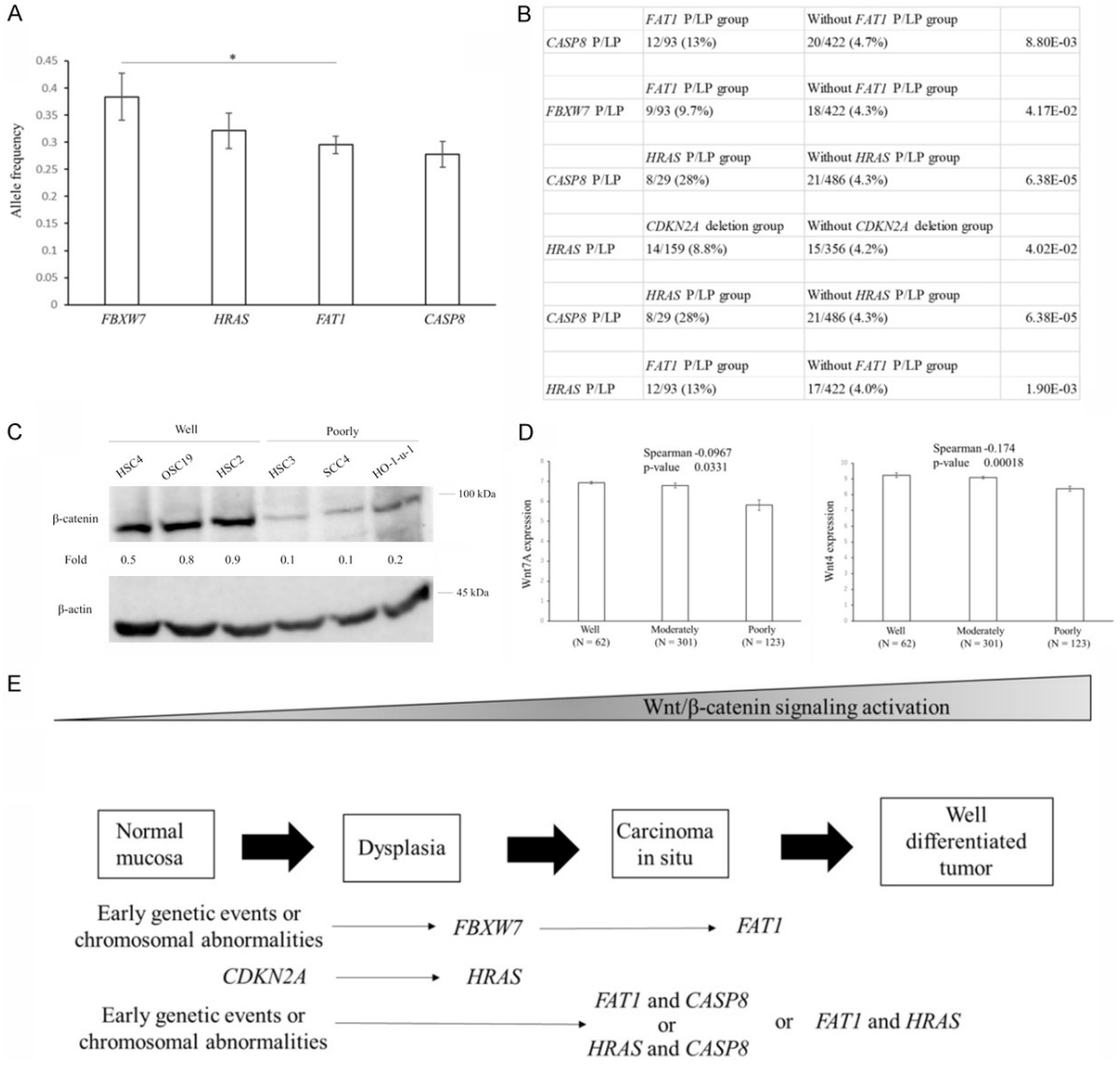

Figure 6. Molecular mechanisms underlying the development of well-differentiated HNSCC. A. The graph shows the allele frequency of P/LP variants in each gene. *P* values for differences in the frequencies of P/LP variants between

genes were generated by the two-sided Student's t-test. B. Pair relationships of genetic changes among P/LP variants or deletions in TCGA HNSCC. Genes with P<0.05 are shown. *P* values were generated by the two-sided Fisher's exact tests. C. Western blots of β-catenin in OSCC cell lines. Band intensities were measured using the software ImageJ. Fold changes relative to the control were calculated using the β-catenin:β-actin ratio. D. Relationship between histological differentiation and Wnt7A or Wnt4 expression in head and neck cancers. The RSEM values for Wnt7A and Wnt4 are shown for head and neck cancers from the TCGA dataset. Data are shown as means ± s.e.m. Wnt7A and Wnt4 expression negatively correlated with histological differentiation using Spearman's rank-based correlation. E. Overview of 5 genes with P/LP variants or deletions significantly enriched in well-differentiated HNSCC. The upper graph depicts the stage and molecular mechanisms throughout tumor development of 5 significantly enriched genes.

Discussion

To the best of our knowledge, this is the first comparative study of metronomic neoadjuvant chemotherapy with S-1 alone for OSCC. We characterized the genetic landscape of OSCC patients who benefit from this treatment. To examine the effectiveness of neoadjuvant chemotherapy, we excluded patients with stage IV OSCC from the analysis. Following the administration of metronomic neoadjuvant chemotherapy with S-1, an increase was observed in the overall survival rate of patients with poorly or moderately differentiated OSCC (93.8% in neoadjuvant chemotherapy versus 50.0% in up-front surgery). Additionally, some P/LP variants in the top-ranked genes were specifically detected in well-differentiated cases, highlighting its effectiveness as a tool for screening in future personalized medicine.

The results showing the survival advantage of metronomic neoadjuvant chemotherapy with S-1 for OSCC will prompt a reconsideration of this treatment, which is not currently recommended in the NCCN guidelines due to the lack of evidence for a survival advantage in randomized trials with neoadjuvant chemotherapy based on MTD [41]. The present results indicate that at least patients with poorly or moderately differentiated OSCC obtain a survival advantage from metronomic neoadjuvant chemotherapy, which supports the implementation of neoadjuvant chemotherapy with S-1 for poorly or moderately differentiated OSCC. Since the development of poorly or moderately differentiated OSCC might be a direct process, spanning occult (not detectable in clinical or imaging examinations) and overt (distant metastasis) stages, metronomic neoadjuvant chemotherapy is beneficial for these patients [42].

The relationship between histological differentiation and chemotherapy or radiotherapy sensitivity is well known. Retrospective studies revealed that patients with poorly or moderately differentiated OSCC were more likely to achieve a pathological complete response after metronomic neoadjuvant chemotherapy [43], which partly explains the survival advantage of poorly or moderately differentiated OSCC patients treated with metronomic neoadjuvant chemotherapy with S-1 in the present study (**Figure 4**). Furthermore, previous studies indicated that patients with poorly or moderately differentiated HNSCC were likely to have various cytokines associated with the immune environment. Metronomic chemotherapy exerts its anti-tumor effects by using immune cells in the tumor microenvironment. The activation of the Wnt pathway in well-differentiated HNSCC suggests that the immune exclusion process by the Wnt pathway [44] needs to be considered in the etiology of well-differentiated HNSCC.

The genes described in the present study are involved in processes that were previously not recognized to play a role in the pathogenesis of well-differentiated HNSCC. The identification of well-differentiated HNSCC-enriched pathogenic variants in *FAT1* broadens the phenotypic spectrum of this gene beyond its currently understood role in Wnt/β-catenin activation [26]. The discovery of high β-catenin expression levels demonstrates that the pathophysiology of well-differentiated HNSCC may begin as early as at the formation of cell adhesion. Additionally, decreases in angiogenesis based on CD31 expression have been reported in an orthotopic nude mouse pancreatic adenocarcinoma (PDAC) model with the overexpression of LCN2 [38], and this study described their histological differentiation-dependent expression, implying that these anti-angiogenic expression patterns are shared in HNSCC and PDAC.

Due to the limitations of a retrospective analysis, the clinical characteristics of the neoadjuvant chemotherapy and up-front surgery groups were not balanced. Beyond these limitations,

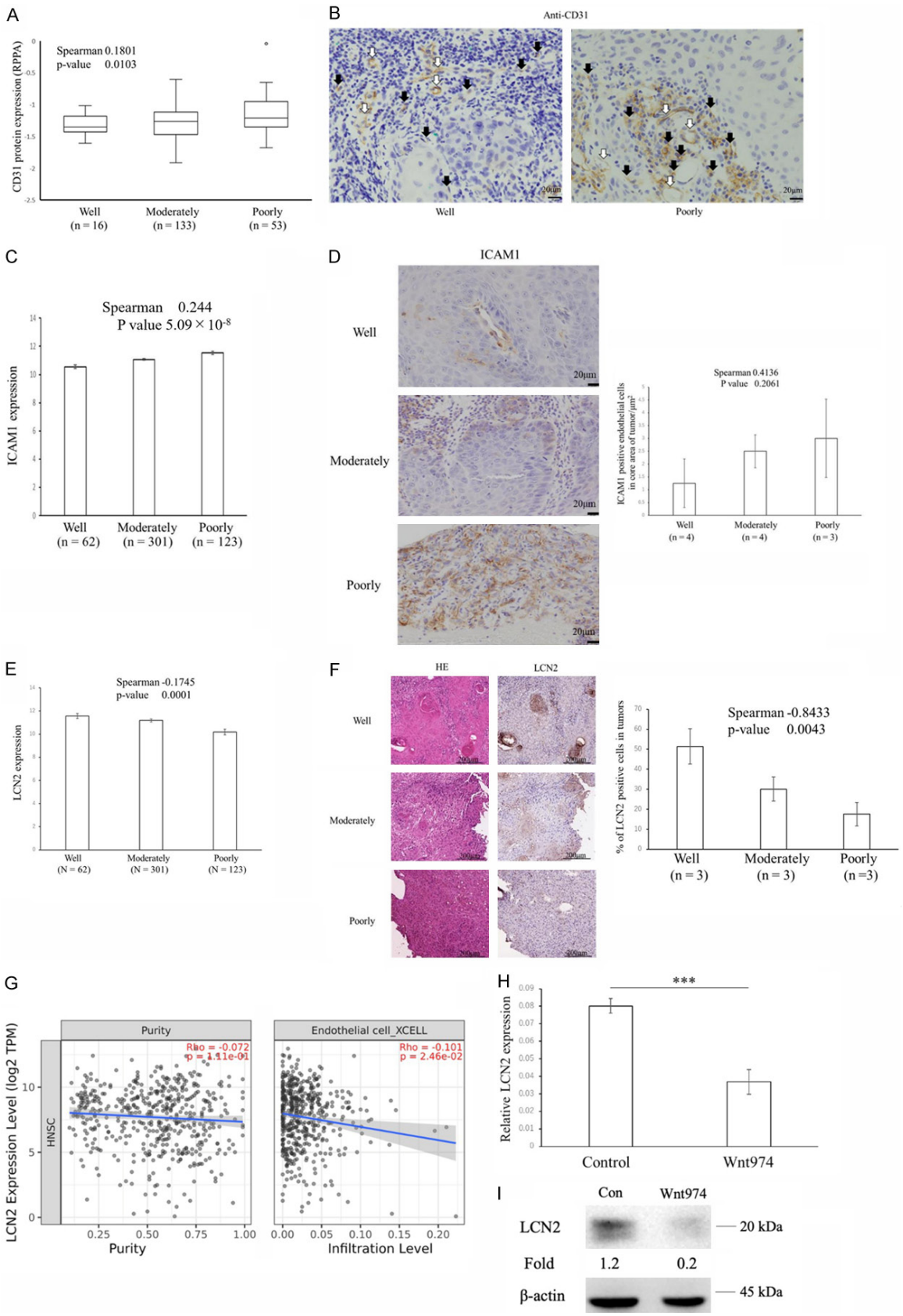

Figure 7. Increases in the angiogenesis suppressor LCN2 in well-differentiated HNSCC. A. Relationship between histological differentiation and CD31 protein expression in head and neck cancers. The Reverse Phase Protein

Array (RPPA) values for CD31 are shown for head and neck cancers from the TCGA dataset. Labels indicate the minimum, 25th percentile, median, 75th percentile and maximum. CD31 expression correlated with histological differentiation using Spearman's rank-based correlation. B. Immunohistochemistry stain of CD31 expression on biopsy sample from a patient with well-differentiated OSCC (left) versus poorly differentiated OSCC (right). White and black arrows denote mature and immature vessel, respectively. C. ICAM1 mRNA expression correlated with histological differentiation using Spearman's rank-based correlation. Data are shown as means ± s.e.m. D. Differences in ICAM1 protein expression in well-, moderately, and poorly differentiated OSCC. Representative histopathology from well-, moderately, and poorly differentiated OSCC stained for ICAM1 (left). Differences in mean ICAM1-positive endothelial cell counts in core area of well-, moderately, and poorly differentiated OSCC are shown (right). Graphs of ICAM1 show the percentages of positive endothelial cells in core of the OSCC at each histological differentiation. Data are shown as means ± s.e.m. The percentage of ICAM1-positive endothelial cells in core area of tumors had mild trends with histological differentiation using Spearman's rank-based correlation. E. LCN2 mRNA expression negatively correlated with histological differentiation using Spearman's rank-based correlation. Data are shown as means ± s.e.m. F. Differences in LCN2 protein expression in well-, moderately, and poorly differentiated OSCC. Representative histopathology from well-, moderately, and poorly differentiated OSCC stained for LCN2 (left). Differences in mean LCN2-positive tumor cell counts in well-, moderately, and poorly differentiated OSCC are shown (right). Graphs of LCN2 show the percentages of positive tumor cells at each histological differentiation. Data are shown as means ± s.e.m. The percentage of LCN2-positive cells in tumors negatively correlated with histological differentiation using Spearman's rank-based correlation. G. Scatterplots of the relationships between LCN2 expression, tumor purity, and the infiltration levels of endothelial cells. Scatterplots are calculated based on the TCGA data of 499 HNSCCs through the 'Gene Module' in Timer2.0. The line in each plot is the fitted linear model. H. Quantification of LCN2 mRNA levels normalized to β-actin (n = 5). Data are shown as means ± s.e.m. The two-sided t-test was used to assess significance. ***P<0.001. OSC19 cells were pretreated with 10 μM Wnt974 for 48 h. I. A Western blot analysis of OSC19 cell lines treated with 10 μM Wnt974 for 2 days. Cell lysates were collected for a Western blot analysis of LCN2 and β-actin. Band intensities were measured using the software ImageJ. Fold changes relative to the control were calculated using the LCN2:β-actin ratio.

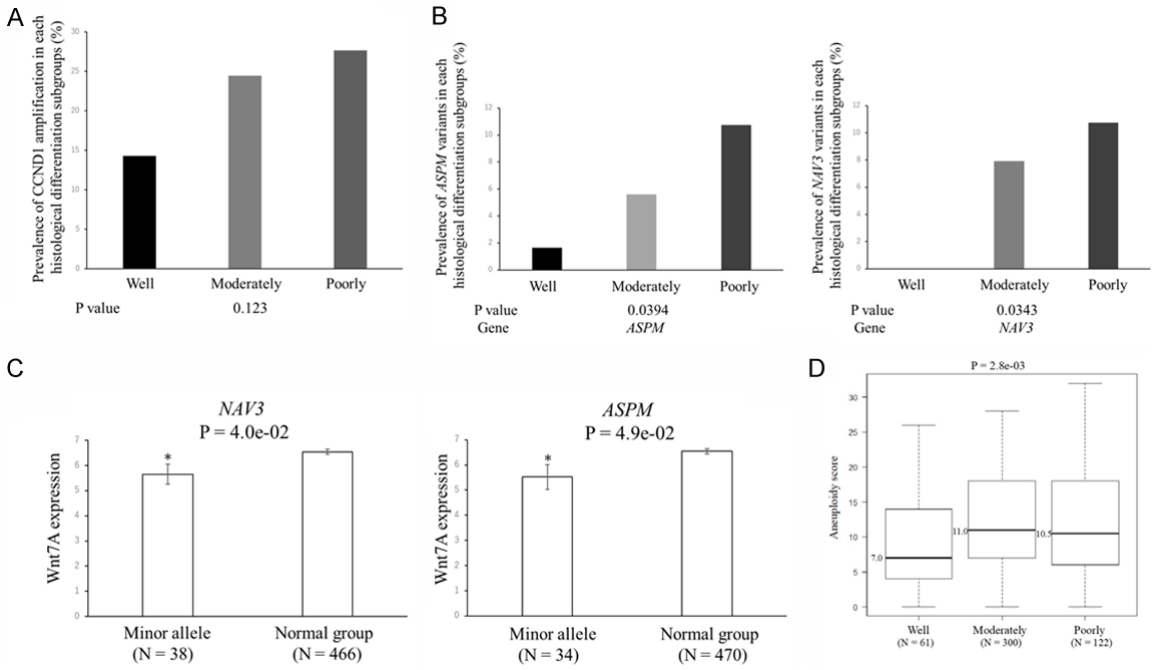

Figure 8. Gene sets associated with poorly differentiated HNSCC. A. The contribution rate of *CCND1* amplification according to the histological differentiation of HNSCC. The rate of *CCND1* amplification between the different types of histological differentiation was calculated from two-sided Fisher's exact tests and generated *P* values. B. The contribution rate of *NAV3* and *ASPM* variants according to the histological differentiation of HNSCC. The rates of *NVA3* and *ASPM* variants between the different types of histological differentiation were calculated from the two-sided Fisher's exact test and generated *P* values. C. Relationship between minor variants and Wnt7A expression in head and neck cancers. RSEM values for Wnt7A are shown for head and neck cancers from the TCGA dataset. Data are shown as means ± s.e.m. A two-sided t-test was used to assess significance. Numbers indicate *P*-values. *P<0.05. D. Aneuploidy scores in patients with well-, moderately, and poorly differentiated HNSCC. We used the Kruskal-Wallis test for comparisons between the different types of histological differentiation. Labels indicate the minimum, 25th percentile, median, 75th percentile, and maximum. N on the x-axis represents the number of patients.

our sample size lacked sufficient statistical power to detect interactions between subgroups (well vs. poorly or moderately). Prospective and multi-institutional studies are crucial for overcoming the limitations of this study and investigating the impact of "metronomic" neoadjuvant chemotherapy on OSCC.

In summary, metronomic neoadjuvant chemotherapy with S-1 alone significantly increased the overall survival rate of patients with poorly or moderately differentiated OSCC, but not those with well-differentiated OSCC. In addition, this study characterized pathogenic variants in well-differentiated HNSCC, broadening the scope of known genes associated with HNSCC and depicting the genetic landscape of HNSCC according to histological differentiation, which will provide insights into common genetic factors in metronomic chemotherapy sensitivity.

Acknowledgements

This work was supported by JSPS KAKENHI Grant Numbers JP21K10084 and 23K16141.

Disclosure of conflict of interest

None.

Address correspondence to: Shinichiro Kina, Department of Medical Education and Development, Graduate School of Medicine, Gunma University, Maebashi, Gunma, Japan. E-mail: kinashin11@gunma-u.ac.jp

References

[1] Kawakita D, Oze I, Iwasaki S, Matsuda T, Matsuo K and Ito H. Trends in the incidence of head and neck cancer by subsite between 1993 and 2015 in Japan. Cancer Med 2022; 11: 1553-1560.

[2] Fu JY, Wu CX, Zhang CP, Gao J, Luo JF, Shen SK, Zheng Y and Zhang ZY. Oral cancer incidence in Shanghai ---- a temporal trend analysis from 2003 to 2012. BMC Cancer 2018; 18: 686.

[3] Dhanuthai K, Rojanawatsirivej S, Thosaporn W, Kintarak S, Subarnbhesaj A, Darling M, Kryshtalskyj E, Chiang CP, Shin HI, Choi SY, Lee SS and Aminishakib P. Oral cancer: a multicenter study. Med Oral Patol Oral Cir Bucal 2018; 23: e23-e29.

[4] Weckx A, Riekert M, Grandoch A, Schick V, Zöller JE and Kreppel M. Time to recurrence and patient survival in recurrent oral squamous cell carcinoma. Oral Oncol 2019; 94: 8-13.

[5] Farnsworth RH, Lackmann M, Achen MG and Stacker SA. Vascular remodeling in cancer. Oncogene 2014; 33: 3496-3505.

[6] Zhong LP, Zhang CP, Ren GX, Guo W, William WN Jr, Sun J, Zhu HG, Tu WY, Li J, Cai YL, Wang LZ, Fan XD, Wang ZH, Hu YJ, Ji T, Yang WJ, Ye WM, Li J, He Y, Wang YA, Xu LQ, Wang BS, Kies MS, Lee JJ, Myers JN and Zhang ZY. Randomized phase III trial of induction chemotherapy with docetaxel, cisplatin, and fluorouracil followed by surgery versus up-front surgery in locally advanced resectable oral squamous cell carcinoma. J Clin Oncol 2013; 31: 744-51.

[7] Bianconi D, Herac M, Posch F, Schmeidl M, Unseld M, Kieler M, Brettner R, Müllauer L, Riedl J, Gerger A, Scheithauer W and Prager G. Microvascular density assessed by CD31 predicts clinical benefit upon bevacizumab treatment in metastatic colorectal cancer: results of the PassionATE study, a translational prospective Phase II study of capecitabine and irinotecan plus bevacizumab followed by capecitabine and oxaliplatin plus bevacizumab or the reverse sequence in patients in mCRC. Ther Adv Med Oncol 2020; 12: 1758835920928635.

[8] do Valle IB, Oliveira SR, da Silva JM, Peterle GT, Có ACG, Sousa-Neto SS, Mendonça EF, de Arruda JAA, Gomes NA, da Silva G, Leopoldino AM, Macari S, Birbrair A, von Zeidler SV, Diniz IMA and Silva TA. The participation of tumor residing pericytes in oral squamous cell carcinoma. Sci Rep 2023; 13: 5460.

[9] Ferdous T, Harada K, Kin T, Harada T and Ueyama Y. Efficacy of schedule-dependent metronomic S-1 chemotherapy in human oral squamous cell carcinoma cells. Int J Oncol 2013; 43: 271-9.

[10] Chen YP, Liu X, Zhou Q, Yang KY, Jin F, Zhu XD, Shi M, Hu GQ, Hu WH, Sun Y, Wu HF, Wu H, Lin Q, Wang H, Tian Y, Zhang N, Wang XC, Shen LF, Liu ZZ, Huang J, Luo XL, Li L, Zang J, Mei Q, Zheng BM, Yue D, Xu J, Wu SG, Shi YX, Mao YP, Chen L, Li WF, Zhou GQ, Sun R, Guo R, Zhang Y, Xu C, Lv JW, Guo Y, Feng HX, Tang LL, Xie FY, Sun Y and Ma J. Metronomic capecitabine as adjuvant therapy in locoregionally advanced nasopharyngeal carcinoma: a multicentre, open-label, parallel-group, randomised, controlled, phase 3 trial. Lancet 2021; 398: 303-313.

[11] Patil V, Noronha V, Menon N, Mathrudev V, Bhattacharjee A, Nawale K, Parekh D, Banavali S and Prabhash K. Metronomic adjuvant chemotherapy evaluation in locally advanced head and neck cancers post radical chemoradiation - a randomised trial. Lancet Reg Health Southeast Asia 2023; 12: 100162.

[12] Ansari MJ, Bokov D, Markov A, Jalil AT, Shalaby MN, Suksatan W, Chupradit S, Al-Ghamdi HS, Shomali N, Zamani A, Mohammadi A and Dadashpour M. Cancer combination therapies by angiogenesis inhibitors; a comprehensive review. Cell Commun Signal 2022; 20: 49.
[13] Goel S, Duda DG, Xu L, Munn LL, Boucher Y, Fukumura D and Jain RK. Normalization of the vasculature for treatment of cancer and other diseases. Physiol Rev 2011; 91: 1071-121.
[14] Porta C, Paglino C, De Amici M, Quaglini S, Sacchi L, Imarisio I and Canipari C. Predictive value of baseline serum vascular endothelial growth factor and neutrophil gelatinase-associated lipocalin in advanced kidney cancer patients receiving sunitinib. Kidney Int 2010; 77: 809-15.
[15] Harada K, Ferdous T and Ueyama Y. Therapeutic strategies with oral fluoropyrimidine anticancer agent, S-1 against oral cancer. Jpn Dent Sci Rev 2017; 53: 61-77.
[16] Hurník P, Režnarová J, Chyra Z, Motyka O, Putnová BM, Čermáková Z, Blažek T, Fománek M, Gaykalova D, Buchtová M, Ševčíková T and Štembírek J. Enhancing oral squamous cell carcinoma prediction: the prognostic power of the worst pattern of invasion and the limited impact of molecular resection margins. Front Oncol 2023; 13: 1287650.
[17] Pickering CR, Zhang J, Yoo SY, Bengtsson L, Moorthy S, Neskey DM, Zhao M, Ortega Alves MV, Chang K, Drummond J, Cortez E, Xie TX, Zhang D, Chung W, Issa JP, Zweidler-McKay PA, Wu X, El-Naggar AK, Weinstein JN, Wang J, Muzny DM, Gibbs RA, Wheeler DA, Myers JN and Frederick MJ. Integrative genomic characterization of oral squamous cell carcinoma identifies frequent somatic drivers. Cancer Discov 2013; 3: 770-81.
[18] Chai AWY, Lim KP and Cheong SC. Translational genomics and recent advances in oral squamous cell carcinoma. Semin Cancer Biol 2020; 61: 71-83.
[19] Sasako M, Sakuramoto S, Katai H, Kinoshita T, Furukawa H, Yamaguchi T, Nashimoto A, Fujii M, Nakajima T and Ohashi Y. Five-year outcomes of a randomized phase III trial comparing adjuvant chemotherapy with S-1 versus surgery alone in stage II or III gastric cancer. J Clin Oncol 2011; 29: 4387-93.
[20] Zhu DW, Liu Y, Yang X, Yang CZ, Ma J, Yang X, Qiao JK, Wang LZ, Li J, Zhang CP, Zhang ZY and Zhong LP. Low Annexin A1 expression predicts benefit from induction chemotherapy in oral cancer patients with moderate or poor pathologic differentiation grade. BMC Cancer 2013; 13: 301.
[21] Inman GJ, Wang J, Nagano A, Alexandrov LB, Purdie KJ, Taylor RG, Sherwood V, Thomson J, Hogan S, Spender LC, South AP, Stratton M, Chelala C, Harwood CA, Proby CM and Leigh IM. The genomic landscape of cutaneous SCC reveals drivers and a novel azathioprine associated mutational signature. Nat Commun 2018; 9: 3667.
[22] India Project Team of the International Cancer Genome Consortium. Mutational landscape of gingivo-buccal oral squamous cell carcinoma reveals new recurrently-mutated genes and molecular subgroups. Nat Commun 2013; 4: 2873.
[23] Martin-Orozco E, Sanchez-Fernandez A, Ortiz-Parra I and Ayala-San Nicolas M. WNT signaling in tumors: the way to evade drugs and immunity. Front Immunol 2019; 10: 2854.
[24] Williams MJ, Werner B, Barnes CP, Graham TA and Sottoriva A. Identification of neutral tumor evolution across cancer types. Nat Genet 2016; 48: 238-244.
[25] Leshchiner I, Mroz EA, Cha J, Rosebrock D, Spiro O, Bonilla-Velez J, Faquin WC, Lefranc-Torres A, Lin DT, Michaud WA, Getz G and Rocco JW. Inferring early genetic progression in cancers with unobtainable premalignant disease. Nat Cancer 2023; 4: 550-563.
[26] Morris LG, Kaufman AM, Gong Y, Ramaswami D, Walsh LA, Turcan Ş, Eng S, Kannan K, Zou Y, Peng L, Banuchi VE, Paty P, Zeng Z, Vakiani E, Solit D, Singh B, Ganly I, Liau L, Cloughesy TC, Mischel PS, Mellinghoff IK and Chan TA. Recurrent somatic mutation of FAT1 in multiple human cancers leads to aberrant Wnt activation. Nat Genet 2013; 45: 253-61.
[27] Hayes TF, Benaich N, Goldie SJ, Sipilä K, Ames-Draycott A, Cai W, Yin G and Watt FM. Integrative genomic and functional analysis of human oral squamous cell carcinoma cell lines reveals synergistic effects of FAT1 and CASP8 inactivation. Cancer Lett 2016; 383: 106-114.
[28] Liu J, Pan S, Hsieh MH, Ng N, Sun F, Wang T, Kasibhatla S, Schuller AG, Li AG, Cheng D, Li J, Tompkins C, Pferdekamper A, Steffy A, Cheng J, Kowal C, Phung V, Guo G, Wang Y, Graham MP, Flynn S, Brenner JC, Li C, Villarroel MC, Schultz PG, Wu X, McNamara P, Sellers WR, Petruzzelli L, Boral AL, Seidel HM, McLaughlin ME, Che J, Carey TE, Vanasse G and Harris JL. Targeting Wnt-driven cancer through the inhibition of Porcupine by LGK974. Proc Natl Acad Sci U S A 2013; 110: 20224-9.
[29] Senthivinayagam S, Mishra P, Paramasivam SK, Yallapragada S, Chatterjee M, Wong L, Rana A and Rana B. Caspase-mediated cleavage of beta-catenin precedes drug-induced apoptosis in resistant cancer cells. J Biol Chem 2009; 284: 13577-13588.
[30] Adorno M, di Robilant BN, Sikandar SS, Acosta VH, Antony J, Heller CH and Clarke MF. Usp16

modulates Wnt signaling in primary tissues through Cdkn2a regulation. Sci Rep 2018; 8: 17506.
[31] Chen Y, Li Y, Xue J, Gong A, Yu G, Zhou A, Lin K, Zhang S, Zhang N, Gottardi CJ and Huang S. Wnt-induced deubiquitination FoxM1 ensures nucleus β-catenin transactivation. EMBO J 2016; 35: 668-84.
[32] Zhang Y and Wang X. Targeting the Wnt/β-catenin signaling pathway in cancer. J Hematol Oncol 2020; 13: 165.
[33] Xie H, Ma Y, Li J, Chen H, Xie Y, Chen M, Zhao X, Tang S, Zhao S, Zhang Y, Du J, Zhang F and Gu L. WNT7A promotes EGF-induced migration of oral squamous cell carcinoma cells by activating β-catenin/MMP9-mediated signaling. Front Pharmacol 2020; 11: 98.
[34] Wang N, Yan H, Wu D, Zhao Z, Chen X, Long Q, Zhang C, Wang X, Deng W and Liu X. PRMT5/Wnt4 axis promotes lymph-node metastasis and proliferation of laryngeal carcinoma. Cell Death Dis 2020; 11: 864.
[35] Guo CR, Han R, Xue F, Xu L, Ren WG, Li M, Feng Z, Hu BC and Peng ZM. Expression and clinical significance of CD31, CD34, and CD105 in pulmonary ground glass nodules with different vascular manifestations on CT. Front Oncol 2022; 12: 956451.
[36] Bhattacharya A, Tóth K, Mazurchuk R, Spernyak JA, Slocum HK, Pendyala L, Azrak R, Cao S, Durrani FA and Rustum YM. Lack of microvessels in well-differentiated regions of human head and neck squamous cell carcinoma A253 associated with functional magnetic resonance imaging detectable hypoxia, limited drug delivery, and resistance to irinotecan therapy. Clin Cancer Res 2004; 10: 8005-17.
[37] Yu L, Maishi N, Akahori E, Hasebe A, Takeda R, Matsuda AY, Hida Y, Nam JM, Onodera Y, Kitagawa Y and Hida K. The oral bacterium Streptococcus mutans promotes tumor metastasis by inducing vascular inflammation. Cancer Sci 2022; 113: 3980-3994.
[38] Huang Z, Zhang Y, Li H, Zhou Y, Zhang Q, Chen R, Jin T, Hu K, Li S, Wang Y, Chen W and Huang Z. Vitamin D promotes the cisplatin sensitivity of oral squamous cell carcinoma by inhibiting LCN2-modulated NF-κB pathway activation through RPS3. Cell Death Dis 2020; 11: 190.
[39] Tong Z, Kunnumakkara AB, Wang H, Matsuo Y, Diagaradjane P, Harikumar KB, Ramachandran V, Sung B, Chakraborty A, Bresalier RS, Logsdon C, Aggarwal BB, Krishnan S and Guha S. Neutrophil gelatinase-associated lipocalin: a novel suppressor of invasion and angiogenesis in pancreatic cancer. Cancer Res 2008; 68: 6100-8.
[40] Pai VC, Hsu CC, Chan TS, Liao WY, Chuu CP, Chen WY, Li CR, Lin CY, Huang SP, Chen LT and Tsai KK. ASPM promotes prostate cancer stemness and progression by augmenting Wnt-Dvl-3-β-catenin signaling. Oncogene 2019; 38: 1340-1353.
[41] Forner D, Noel CW, Wu V, Parmar A, Chan KKW, de Almeida JR, Husain Z and Eskander A. Non-surgical management of resectable oral cavity cancer in the wake of COVID-19: a rapid review and meta-analysis. Oral Oncol 2020; 109: 104849.
[42] Farrokhian N, Holcomb AJ, Dimon E, Karadaghy O, Ward C, Whiteford E, Tolan C, Hanly EK, Buchakjian MR, Harding B, Dooley L, Shinn J, Wood CB, Rohde SL, Khaja S, Parikh A, Bulbul MG, Penn J, Goodwin S and Bur AM. Development and validation of machine learning models for predicting occult nodal metastasis in early-stage oral cavity squamous cell carcinoma. JAMA Netw Open 2022; 5: e227226.
[43] Kina S, Kawabata-Iwakawa R, Miyamoto S, Kato T, Kina-Tanada M and Arasaki A. EphA4 signaling is involved in the phenotype of well-differentiated oral squamous cell arcinoma with decreased tumor immunity. Eur J Pharmacol 2023; 945: 175611.
[44] Luke JJ, Bao R, Sweis RF, Spranger S and Gajewski TF. WNT/β-catenin pathway activation correlates with immune exclusion across human cancers. Clin Cancer Res 2019; 25: 3074-3083.